Meteorol Atmos Phys (2007)
DOI 10.1007/s00703-006-0243-2
Printed in The Netherlands

Meteorology and Atmospheric Physics

[1] Department of Meteorology, The Pennsylvania State University, PA, USA
[2] Hurricane Research Division, NOAA/AOML, Miami, FL, USA

Comparison of observed gale radius statistics

A. C. Moyer[1], **J. L. Evans**[1], and **M. Powell**[2]

With 12 Figures

Received August 10, 2006; accepted September 11, 2006
Published online: March 14, 2007

Summary

Forecasts of tropical cyclone track and intensity have long been used to characterize the evolution and expected threat from a tropical storm. However, in recent years, recognition of the contributions of subtropical cyclogenesis to tropical storm formation and the process of extratropical transition to latter stages of the once-tropical storm's lifecycle have raised awareness about the importance of storm structure. Indeed, the structure of a cyclone determines the distribution and intensity of the significant weather associated with that storm.

In this study, storm structure is characterized in terms of significant wind radii. The radii of tropical storm, damaging, and hurricane-force winds, as well as the radius of maximum winds are all analyzed. These wind radii are objectively derived from the H*Wind surface wind analysis system. Initially, six years of these data are examined for consistency with previous studies. Having ascertained that the H*Wind radii are realistic, detailed comparisons are performed between the H*Wind and NHC Best Track wind radii for two years (2004 and 2005) of North Atlantic tropical storm and hurricane cases. This intercomparison reveals an unexpected bias: the H*Wind radii are consistently larger than the NHC Best Track for all but the smallest and least intense storms.

Further examination of the objectively-determined H*Wind tropical storm force wind radius data compared to subjectively-determined radii for the same storm times demonstrates that the objective wind radii are *underestimating* the extent of the tropical storm force wind area. Since the objective H*Wind radii are large compared to the NHC Best Track – and yet underestimate the area of tropical storm force winds – this argues for further examination of the methods used to ascertain these significant wind radii.

1. Introduction

Tropical cyclones cause great loss to life and property in all basins where they develop. In spite of the sophisticated forecasting and mitigation strategies in the United States, hurricanes cause an average of $5 billion in damage annually (Pielke and Landsea, 1998). Individual events and years can be far more devastating than this average number implies (e.g., Katrina and other 2005 storms; White House, 2006). Currently, tropical storm and hurricane warnings are issued for an average of 570 km of coastline per storm (Marks and Shay, 1998). These warnings rely implicitly on knowing the storm's future track as well as its area, or radial extent, of key wind thresholds. Although track forecasts have improved dramatically in the last decade, the average length of coastline warned has not been concomitantly reduced since forecasters have the least confident in forecasts of outer wind radii (J. Franklin, personal communication 2005).

Improvements in forecasts of outer wind radii could provide societal benefits (e.g., additional guidance for local emergency managers for landfalling hurricanes). Such wind radii forecasts would most likely include 17 m s^{-1} (radius of tropical storm force winds, R_{TS}), 26 m s^{-1} (radius of "damaging" winds, R_{DAMG}), 33 m s^{-1} (radius of hurricane force winds, R_{HURR}), and the radius

of maximum winds, R_{MAX}. A number of historical datasets of these wind radii for North Atlantic tropical storms and hurricanes are presently available from (i) the ''extended best-track'' (EBT) data set (Pennington et al, 2000), (ii) the NOAA Hurricane Research Division (HRD) H*Wind Application (Powell et al, 1998), as well as (iii) the National Hurricane Center's (NHC) post storm analyzes beginning in 2004 (*ftp://ftp.nhc.noaa.gov/pub/atcf/*). Currently, the National Hurricane Center determines outer wind radii using three types of data: surface observations, aircraft reconnaissance data, and satellite-derived winds (J. Franklin, personal communication 2005). Unfortunately, the surface observation network over the ocean is limited to floating and moored buoys and passing ships (the last of which, for obvious reasons, avoid hurricanes). Use of aircraft reconnaissance data also has limitations, because of the debate over the appropriate adjustment factor to determine surface winds from flight level winds. Also, since the areal extent of the aircraft reconnaissance is most focused on the storm position and intensity, the outer wind radii are often not well sampled by the aircraft, especially for large storms. Satellite derived winds, like those from QuikSCAT, appear to hold the most promise for elucidating outer wind radii, but the radiometers on the satellite currently have a problem penetrating deep layers that are precipitating. Further, these sensors are on polar orbiting satellites and so their temporal sampling of a particular location is limited.

The EBT data set of Pennington et al (2000) was compiled from operational wind radii advisories issued by NHC from 1988 through the present. Thus, the wind radii characteristics between this dataset and the National Hurricane Center's (NHC) post storm analyzes beginning in 2004 are expected to be consistent. Kimball and Mulekar (2004) showed that the EBT set was consistent with theory concerning size of tropical cyclones. Their analysis of the EBT was one of the primary motivations for this study. Kimball and Mulekar ran statistical tests on a variety of different parameters within the EBT, and also stratified their data by some of the same parameters used in later sections of this study (e.g., Saffir–Simpson Scale, intensity change, etc.). While Kimball and Mulekar considered different wind radii (such as eye radius and radius of maximum winds) than are focused on here, their study provides a framework for comparison of the H*Wind and NHC Best Track wind radii datasets.

The Hurricane Research Division H*Wind application (Powell and Houston, 1996; Powell et al, 1998) analyzes the surface wind field of a tropical cyclone, providing both gridded data and a graphical display as output. The R_{TS}, R_{DAMG}, and R_{HURR} radii values for four quadrants (NW, NE, SE, SW), as well as the radius of maximum winds and maximum wind speed, are given on the plots of the wind field. This is an advantage over the single values for radii in each quadrant given by NHC, as the H*Wind maps provide context for the wind radii. An outline of the H*Wind methodology for determining surface winds is given in Sect. 2.

Demuth et al (2004) attempt to estimate outer wind radii (among other parameters) using the Advanced Microwave Sounding Unit (AMSU). Their algorithm derives the wind field using temperature, pressure, and upper-level wind values. These values are then used in multiple linear regressions to determine the outer wind radii. However, in developing the regression equations, the Extended Best Track (EBT) was used as a training set. This introduces a bias toward NHC operational values for the wind radii and is not a fully independent set of the EBT itself. While this data is useful to hurricane forecasters, it cannot be used as another independent data set to compare alongside of the NHC Best Track and H*Wind.

Kossin et al (2006) developed a satellite-based tool for determining Atlantic tropical cyclone outer wind radii. In their approach, geostationary satellite data are used to determine R_{MAX} directly and principal component analysis is utilized to determine the outer wind radii from R_{MAX} and the cloud signature in the infrared satellite picture. However, in developing the principal component analysis, Kossin et al (2006) employed the NHC Best Track data as the training set, similar to Demuth et al (2004). Naturally, the results from Kossin et al (2006) are somewhat biased toward what the NHC values for outer wind radii.

The analysis presented here looks to first determine if the outer wind radii data in H*Wind are consistent with previous published theory and observations and then to compare the data in H*Wind to that of the NHC post storm analyzes. In the following sections, a description of the sta-

tistical tools used to analyze the datasets is provided. The results and discussion follow, with an emphasis on the differences between the NHC and H*Wind datasets and potential sources for these differences. Finally, a look to the future of outer wind radii forecast tools concludes the study.

2. Methods

In this section, details of dataset construction and methods of comparison of datasets are discussed. Both subjective and objective techniques were used to contrast the datasets examined in this study. These procedures include histograms, boxplots, hypothesis testing, and regression analysis. The outcomes of these comparisons will be discussed in Sect. 3.

In addition to their forecasting responsibilities, the National Hurricane Center (NHC) in Miami, FL is responsible for maintaining historical records of tropical cyclones in the Atlantic and East Pacific basins. Their ''best track'' records for Atlantic storms are compiled in the North Atlantic hurricane database (HURDAT). Within HURDAT, well known variables such as minimum sea-level pressure, maximum surface wind speed, and location are recorded going back to 1851. Beginning in 2001, NHC added gale radius to the best track and in 2004 the 50 kt ($26\,m\,s^{-1}$) and hurricane force wind radii were added as well. Also in 2004, NHC began to perform post storm analyzes on their forecast values of the outer wind radii. The NHC best track data used in this study are from the 2004 and 2005 seasons. The dataset for this study was collected by concatenating the NHC best track files into one file and then importing that file into Microsoft Excel.

*2.1 Outline of H*Wind procedure*

The Hurricane Research Division (HRD) uses a different approach for obtaining information about the wind field of a hurricane. The HRD H*Wind surface wind analysis system amasses available surface (10 meter) and near-surface observations and utilizes an objective analysis procedure (Ooyama, 1987) to analyze the spatial distribution of the surface wind field. H*Wind analyzes have been produced since 1994. A user of the H*Wind analysis system looks at the surface wind radius data and performs quality control on the data. Observation platforms include, but are not limited to: aircraft reconnaissance, SFMR (Stepped Frequency Microwave Radiometer), ship and buoy observations, FCMP tower array, C-MAN observing platforms, some ASOS data, GOES cloud drift analyzes, and QuikSCAT passes. In the quality control process, the user looks for inconsistent observations and removes (or flags) them from the analysis. For example, given two collocated observations, one from flight level data reduced to the surface and the other from the SFMR, the user would flag the flight level observation, because it has a higher variance than the SFMR observation. Occasionally, if data for a particular analysis is sparse, a synthetic vortex is added to the analysis based on the previous H*Wind analysis. After the user quality controls all input data, objective analysis is used to interpolate between data points using a cubic B-spline (Ooyama, 1987). Once the objective analysis is performed, H*Wind contours the wind field and a series of graphics covering various storm-centered domains (2°, 4°, and 8° from the storm center) are produced.

In order to assess the validity of the H*Wind dataset, as well as to compare the H*Wind outer wind radii data to the NHC post storm reanalyzes, a dataset was manually created by transcribing the data from each individual image into Microsoft Excel. This data set includes data from the 2000 to 2005 hurricane seasons. Six hundred and ninety-one H*Wind analyzes from 59 storms in the six year period were included in this database.

*2.2 Considerations in statistical analysis of the H*Wind wind radii*

Graphical techniques such as boxplots and histograms were applied to the data in order to get a qualitative description of the data. A variety of hypothesis tests were used on the H*Wind data, including analysis of variance (ANOVA) and Student's *t*-tests. Regression analysis was utilized to compare the NHC gale radii to the H*Wind gale radii.

Regression analyzes are not robust to datasets with large serial correlation. In order to remove the serial correlation from the datasets, a resampling without replacement technique was employed. The resampling method consisted of

randomly sampling i individual storm times from each storm from $i = 1$ to 10 and creating 100 new datasets for each i. That is, there were 100 datasets that had exactly one observation of each storm in it, although that observation was not intended to be the same in each set. There were 100 more datasets that had exactly two observations from each storm, assuming that there were two observations available for each storm. This continued until 10 observations were being sampled from each storm. The average number of observations per storm was 13. Regression analysis was then performed on each of the 1000 new datasets resulting from this storm sub-sampling. Although there is not a rigorous test to prove its validity, it is assumed if the range of the coefficients of the linear regression analysis is small and the mean of the coefficients is similar to the original coefficient, then serial correlation is not adversely affecting the original regression analysis.

3. Results and discussion

The characteristics of the H*Wind outer wind radii data set have never before been analyzed to determine whether they are physically realistic. An analysis of the veracity of H*Wind gale radii must be completed to demonstrate its usefulness before making any comparisons to the NHC outer wind radii.

*3.1 Validity of the H*Wind data set*

In this section, it will be shown through multiple statistical analyzes on many different variables that the H*Wind data set is indeed physically reasonable. R_{TS}, R_{DAMG}, R_{HURR}, R_{MAX} are the measures of the surface wind structure used in this study, although the results from R_{TS} are emphasized. These wind radii measures are partitioned according to storm category (i.e., Saffir Simpson scale), intensity change, land interaction (prior to landfall, over land and return over water) and latitude to determine the storm structure changes implied in each partition. These changes are evaluated for their consistency with theory and with previous statistical studies of the historical data.

Histograms of the R_{TS}, R_{DAMG}, and R_{HURR}, outer wind radii as well as the radius of maximum winds (R_{MAX}) for all storms in the H*Wind data set are plotted in Fig. 1. The R_{TS} and R_{DAMG}

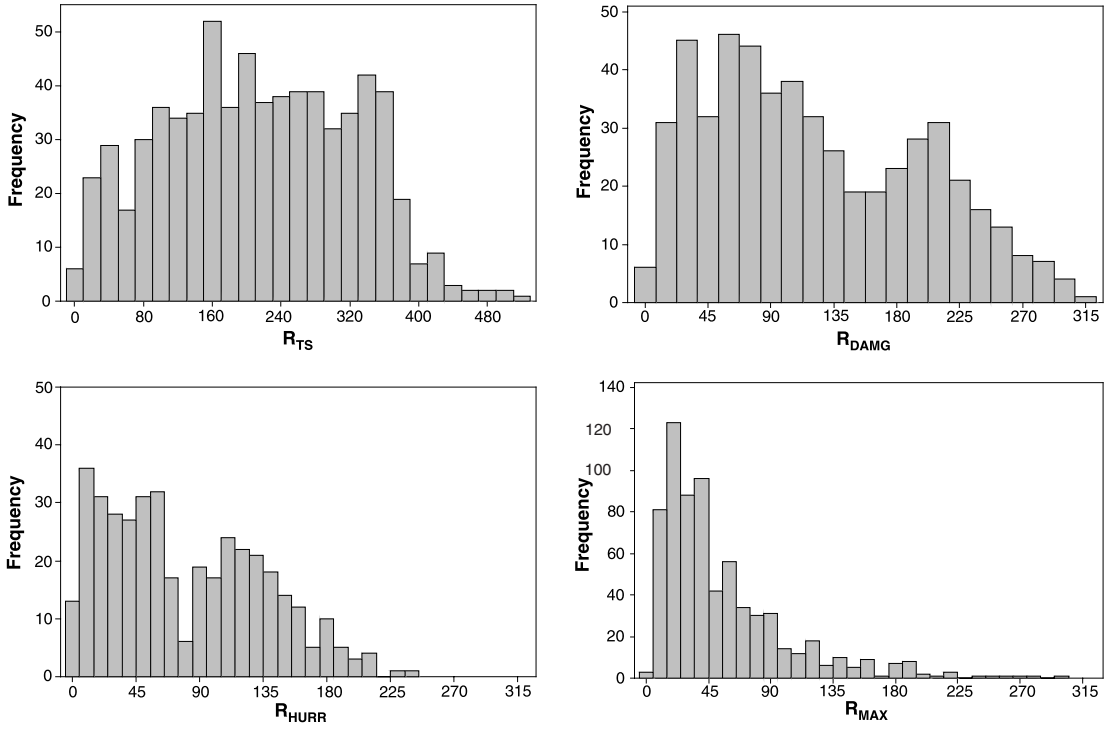

Fig. 1. Histograms of R_{TS} (top left), R_{DAMG}(top right), and R_{HURR} (bottom left) as well as radius of maximum winds (bottom right). The values of the wind radii are in kilometers. Note that the scale for R_{TS} is different than the other plots. The total number of storm times contributing to each frequency plot is listed in Table 1

histograms do not show strong skewness to either the left or the right; the R_{HURR} histogram is slightly left skewed; and the histogram for the radius of maximum winds is highly left skewed. These results are consistent with theory: the R_{TS} and R_{DAMG} are often found outside the core of the tropical cyclone. Since there is a large spectrum of tropical cyclone sizes, it is not surprising that these two radii do not show skewness. On the other hand, for 30% of the hurricanes (all 122 H1 of the subset of 397 hurricane times) the R_{HURR} radius is within the core of the cyclone. Since the dynamics of the inner core are vastly different than that of the outer core (e.g., Weatherford and Gray, 1988), it is not surprising that two different distributions would describe the data. When combined, this would give the appearance of left skewed data. Interestingly, since the H*Wind dataset has many more tropical storms than any other category (Table 1), one might think that the R_{TS} and R_{DAMG} radii may be left skewed as well. However, tropical storms come in variety of sizes, and those that form subtropically or are undergoing extratropical transition often have very large wind fields. The mean and standard deviation for R_{TS} derived from H*Wind are similar to those obtained by Kimball and Mulekar (2004), however, the means and standard deviations of R_{DAMG} and R_{HURR} are significantly smaller in this study when compared with Kimball and Mulekar.

Table 1. Descriptive statistics for the H*Wind dataset. The sample size is given by n, the means by $\bar{x}$, and the standard deviation by s. The subscripts denote the outer wind radii for which the statistics are applicable

	All	TS	H1	H2	H3	H4	H5
n	691	294	122	90	99	78	8
$\bar{x}_{17}$	213.7	137.9	215.8	298.0	295.5	288.6	279.9
s_{17}	109.5	92.8	79.1	79.6	66.7	80.0	52.5
$\bar{x}_{26}$	92.7	22.1	95.4	168.9	165.3	165.2	131.5
s_{26}	86.2	34.8	55.6	71.7	64.3	65.3	58.3
$\bar{x}_{33}$	45.2	–	34.4	97.9	100.4	101.5	73.6
s_{33}	57.5	–	38.1	54.5	48.1	49.0	32.0

For mature tropical cyclones, the radius of maximum winds (R_{MAX}) is near the center of circulation in the eyewall. It makes sense, then, that most of the values of the radius of maximum winds are small. Cases where the radius of maximum winds would not be near the center of the cyclone are during eyewall replacement cycles (Willoughby, 1982), as well as incipient cyclones that are still developing a central core, and subtropical storms.

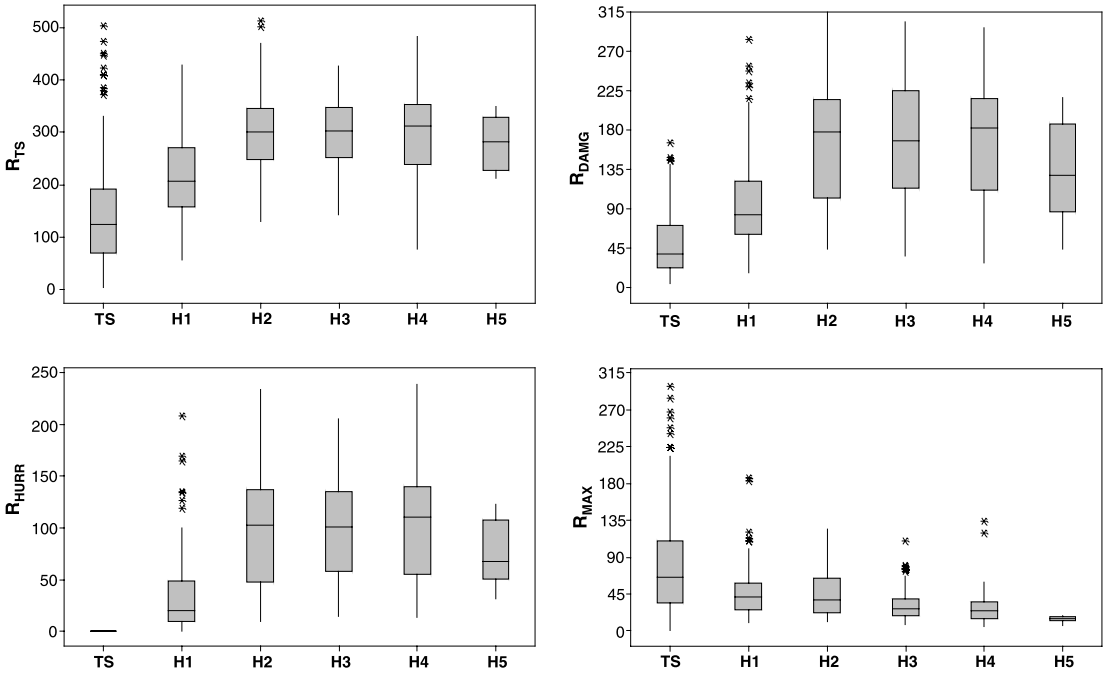

Fig. 2. Boxplots stratified by Saffir–Simpson category of R_{TS} (top left), R_{DAMG} (top right), and R_{HURR} (bottom left) as well as radius of maximum winds (bottom right). The wind radii are in kilometers. Note that the scale of R_{TS} is different from the other plots

(a) H*Wind Stratification by Saffir–Simpson Category

Boxplots (stratified by Saffir–Simpson category) for each of the three outer wind radii measures and R_{MAX} illustrate that tropical storms have the smallest median R_{TS}, followed by Category 1 hurricanes. Category 2, 3, and 4 hurricanes had nearly identical medians, and Category 5 storms had a slightly smaller median the Category 2, 3, and 4 storms (Fig. 2). The spread and left-skewed nature of the values for tropical storms' R_{TS} is most likely due to the different types of storms that fit into the tropical storm category. Storms that formed subtropically or were undergoing extratropical transition generally had much larger R_{TS}, due to their synoptic environment. The variance for the Category 1, 2, 3, and 4 hurricanes are roughly the same, and the variance for the Category 5 storms is smaller than the other category hurricanes due to its very small sample size (Table 1).

For R_{DAMG}, a similar pattern emerges. Tropical storms still have the smallest R_{DAMG} median, followed by Category 1 hurricanes. Category 2, 3, and 4 hurricanes have similar medians for R_{DAMG}, and Category 5 storms have a slightly smaller median (Fig. 2). Tropical storms and Category 1 hurricanes are left skewed, with outliers at large values for R_{DAMG}. Category 2, 3, and 4 hurricanes have similar spread, while Category 5 storms again have less variance. This result is similar to the results from Weatherford and Gray (1988a, b) who showed that in the Western North Pacific, outer core strength (defined as the areally averaged 1°–2.5° wind speed) is not related to central pressure.

The R_{HURR} data do not show much difference from the outer wind radii. Category 1 hurricanes have the smallest median R_{HURR}, while Category 2, 3, and 4 storms have similar medians for their R_{HURR}. Category 5 hurricanes again have smaller R_{HURR} than the Category 2, 3, and 4 hurricanes. It is hypothesized that the Category 5 hurricanes have smaller outer wind radii than the middle three categories due to the compact nature of Category 5 hurricanes (e.g., Ho et al, 1987), which usually can only be sustained for up to two days and are usually the result of rapid intensification, where the pressure gradient is especially strong near the center of circulation. The Category 1 hurricanes for R_{HURR} are again left skewed, with outliers at large values, greater than 1.5 times the IQR. Category 2, 3, and 4 hurricanes have similar variance, and Category 5 storms have smaller variance. Overall, the outer wind radii profiles from H*Wind for each Saffir–Simpson category appear to be consistent with Kimball and Mulekar (2004, their fig. 20).

The radius of maximum winds statistics for H*Wind are consistent with theory and with the results of Kimball and Mulekar (2004). Willoughby (1982) hypothesized that winds increase in a hurricane by conservation of angular momentum. This would result in broader, weaker storms with decreasing radius of maximum wind as the peak wind speed increased. Tropical storms had the largest median radius of maximum winds and also the largest spread of the H*Wind data sampled here. As storm intensity increases, each successive category's median gets smaller with less spread, culminating in Category 5 storms with mean R_{MAX} less than 20 km. The boxplot for the radius of maximum wind data is strikingly similar to that given in Kimball and Mulekar (2004; their fig. 15).

For the rest of this paper, only the gale radius will be examined. The reasons for this are twofold. First, the results of the remaining tests show the most statistical significance for the R_{TS} statistics. Also, the same trends that are apparent in the R_{TS} data appear in the data for the other outer wind radii, however, the trends are not as strong. Thus, for the sake of brevity only the R_{TS} results are reported here. The complete analysis of all wind radii is available in Moyer (2006).

(b) H*Wind Stratification by Intensity Change

The relationship between R_{TS} and the storm intensity tendency is examined here. Intensity change is defined as a 2.5 m s^{-1} (5 kt) change in the maximum wind speed over 6 hours. Thus, a storm whose wind speed dropped 2.5 m s^{-1} in 6 hours was categorized as "decaying," while a storm whose peak winds did not vary more than $\pm$2.5 m s^{-1} in 6 hours was classified "little change" and a storm with an increase in maximum wind speed of 2.5 m s^{-1} in 6 hours was considered "strengthening". If there was more than 12 hours between consecutive observations, the tendency was not calculated across this time window. This classification was used for all storms

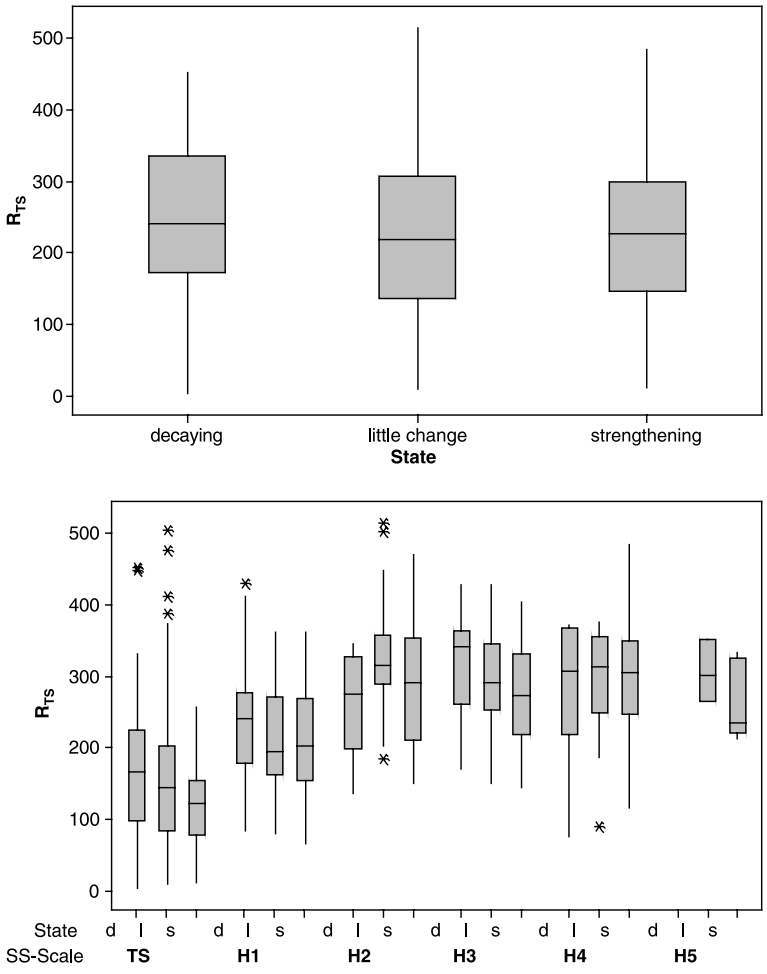

Fig. 3. Boxplots of R_{TS} separated by "state" (i.e., intensity tendency) for all storms (top) and further separated by Saffir–Simpson category (bottom)

and then partitioned into storms in each individual Saffir–Simpson category based on their final intensity (i.e., if the storm weakened from a Cat 3 to a Cat 2, it would be classified in the Cat 2 set for this analysis).

Boxplots of R_{TS} for all storms vs. state and for storms separated by Saffir–Simpson category and state are plotted in Fig. 3. An ANOVA was performed on the data to determine whether differences in the means of each classification are significant (Table 2). While the unstratified (all storms) set did not show a significant response to state, gale radius showed a statistically significant response to intensity change for tropical storms and Category 2 storms, and the relationship for Category 3 storms was marginal. Croxford and Barnes (2002) showed for Atlantic storms that inner core strength (defined as the mean tangential wind speed in the annulus from 60 to 145 km radius) is related to intensity change. The results for R_{HURR} presented in Moyer (2006) display a similar phenomenon. Inspection of the boxplots reveals that storms that are decaying have larger R_{TS} than storms that are strengthening. This is most apparent in the tropical storm and Category 3 storms.

Table 2. P-values from ANOVA tests stratified by Saffir–Simpson category for intensity change, land interaction, and latitude

Storm category	Intensity change	Land interaction	Latitude
All	0.432	0.000	0.001
TS	0.025	0.000	0.003
H1	0.396	0.226	0.007
H2	0.013	0.366	0.000
H3	0.079	0.017	0.000
H4	0.922	0.010	0.135

(c) H*Wind Stratification by Land Interaction

The impact of land interaction on outer wind radii was the next mode of stratification. All

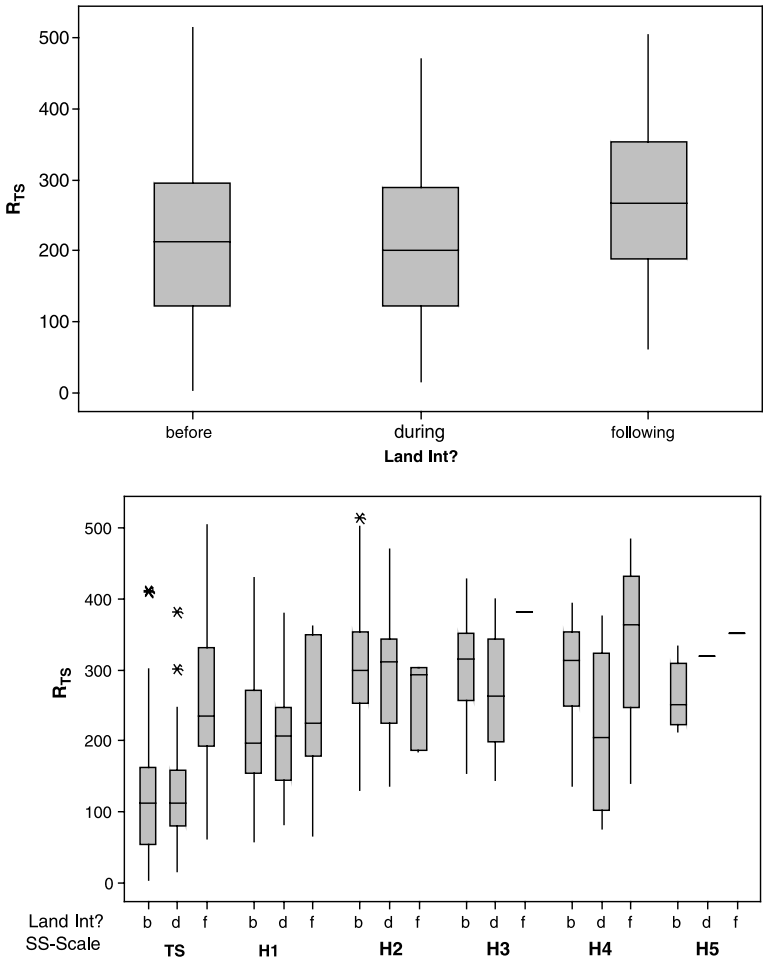

Fig. 4. Boxplots of R_{TS} separated by interaction with land for all storms (top) and further separated by Saffir–Simpson category (bottom)

storms were classified as ''before'' land interaction, ''during'' land interaction, or ''following'' land interaction. If a storm moved back over open water, the storm was classified as before land interaction once it regained its inner core. As with intensity change, ANOVA tests were performed on the entire dataset, as well as each Saffir–Simpson category.

The results of this analysis are given in Table 2 for all wind radii along with the accompanying boxplot in Fig. 4 for R_{TS}. The effects of land interaction are statistically significant for the all storms dataset, and for the subsets of tropical storms and Category 4 hurricanes. The effects of land interaction appear to increase R_{TS} following interaction with land. Category 3 hurricanes have a significant *p*-value, however only one storm in the dataset was a Category 3 hurricane following a land interaction, so there is little merit in this small *p*-value. Category 1 and 2 hurricanes did show a statistically significant effect from land interaction.

(d) H*Wind Stratification by Latitude

The final parameter used to judge the validity of the H*Wind dataset is the variation of the wind radii with latitude. Previous observational studies have shown that wind fields tend to increase in size with latitude (e.g., Kimball and Mulekar, 2004). The H*Wind dataset is consistent with this previous work. Once again ANOVA tests were performed to compare the means of the various wind radii across different latitude bands and partitioned across the Saffir–Simpson categories. The latitude bands chosen are listed in Table 3.

For R_{TS}, the variation of radius with latitude was statistically significant for all storms and all categories of storms except for Category 4 hurri-

Table 3. Latitude bands used for stratifying ANOVA test

Southern latitude (°N)	10.1	15.1	20.1	25.1	30.1	35.1
Northern latitude (°N)	15.0	20.0	25.0	30.0	35.0	40.0

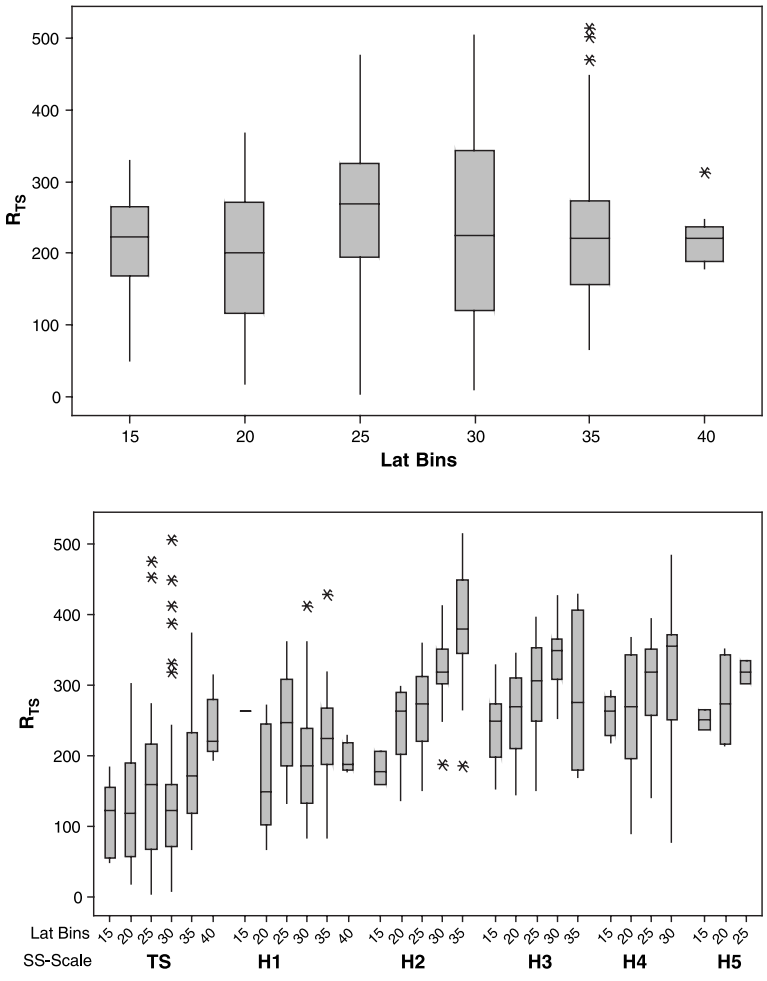

Fig. 5. Boxplots of R_{TS} separated by latitude for all storms (top) and further separated by Saffir–Simpson category (bottom)

canes (Table 2). The boxplots of the Category 4 hurricanes exhibit a large variance in R_{TS} at different latitude, making it difficult to find a significant result from the ANOVA test (Fig. 5). In general, as storms move further northward, their R_{TS} increases.

*3.2 Analysis of H*Wind compared to NHC Best Track wind radii*

Having ascertained that the H*Wind dataset is consistent with theory and previous statistical studies of storm wind radii variations, it is now valuable to consider how well this dataset agrees with the other readily available wind radii dataset, the NHC Best Track dataset, and to investigate the sources of any discrepancies. Throughout the remainder of these analyzes, only the 2004 and 2005 seasons are considered since in these seasons the NHC hurricane specialists performed post-season analyzes on their operational wind radii estimates. Thus, the comparison of H*Wind and the NHC Best Track wind radii is restricted to 23 storms (consisting of 303 individual storm times) from the 2004 and 2005 North Atlantic hurricane seasons.

(a) Initial Intercomparison of H*Wind and NHC Best Track Gale Radii

A scatterplot with a regression line and a 1-to-1 line for all the storms that have concurrent times in the NHC and H*Wind datasets is displayed in Fig. 6. The regression equation obtained from these data is given by

$$\mathrm{NHC17} = 39.7 + 0.672^{*}\mathrm{HWIND17},$$

where NHC17 is the value of the $17\,\mathrm{m\,s^{-1}}$ radius in the NHC Best Track dataset and HWIND17 is the value of the $17\,\mathrm{m\,s^{-1}}$ radius (R_{TS}) in the H*Wind dataset. A hypothesis test was performed on whether the slope coefficient is significantly different from one and it returned a p-value of 0.000. Thus, the slope of the regression is differ-

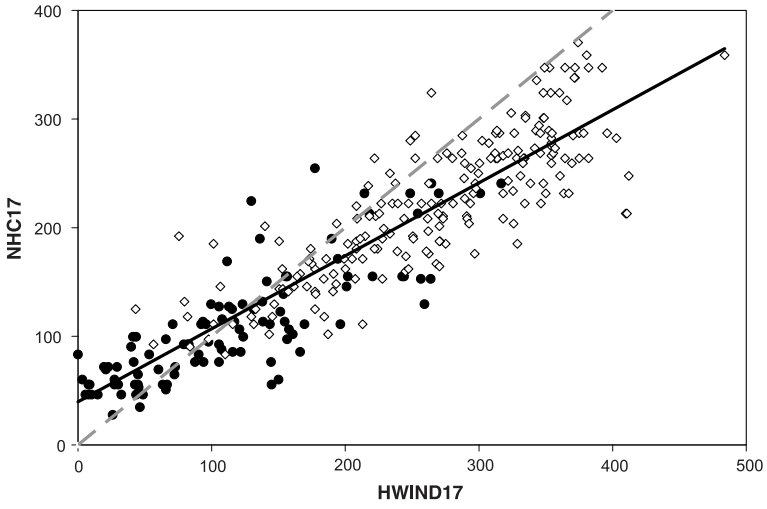

Fig. 6. Scatterplot of R_{TS} from the NHC Best Track vs. the H*Wind dataset for concurrent storm times from 2004 to 2005 with black regression line and gray dashed 1:1 line plotted. The black circles indicate tropical storms

ent from one, and it is clear that there are systematic differences between NHC and H*Wind analyzes when all storm categories are considered together.

A paired *t*-test was used to determine if the significant differences evident between the means of the two complete datasets are preserved when the storms are partitioned into Saffir–Simpson categories (Table 4). Based on these *t*-tests, with the exception of tropical storms, all Saffir-Simpson categories have significant differences in their means. The tropical storms in the two datasets were not significantly different than zero because most of the observations fell near the one-to-one line, although there was some spread in the data (Fig. 6). Boxplots of the differences between the two datasets stratified by storm category are shown in Fig. 7: with the exception of TS, H*Wind consistently has larger R_{TS} than NHC analyzes.

Table 4. Results (*p*-values) from *t*-tests for differences in the means of H*Wind and NHC R_{TS} stratified by storm Saffir Simpson category. The first two columns (from left to right) are all storms and a long-lived subset of storms (Hurricanes Charley, Frances, Ivan, Jeanne, Katrina, Rita, and Wilma from 2004 and 2005). Paired *t*-tests were used to compare these results. Results of a comparison between the H*Wind and NHC R_{TS} stratified by the presence or absence of a QuikSCAT overpass are given in the final column. For this analysis, two-sample *t*-tests are used to compare the differences in the means of H*Wind and NHC R_{TS} when there was/was not QuikSCAT data available in the H*Wind analysis

Storm category	All storms	Storm subset	QuikSCAT
All	0.000	0.000	0.122
TS	0.263	0.965	0.662
H1	0.000	0.014	0.680
H2	0.000	0.000	0.258
H3	0.000	0.000	0.299
H4	0.000	0.000	0.087

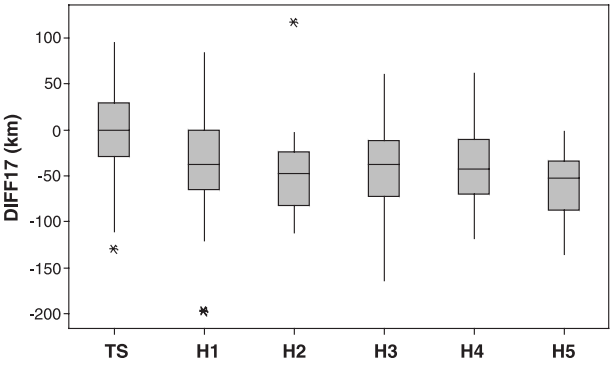

Fig. 7. Boxplots of DIFF17, the difference between NHC and H*Wind (NHC-H*Wind) analyzed R_{TS} separated by Saffir–Simpson category

(b) Exploration of the Effect of Long-lived, Intense Storms

In the course of the analysis, it appeared that weak and/or short lived storms had the largest differences between the two datasets. To determine if these short-lived, weak storms were causing bias in the data, the regression analysis was re-examined using only strong, long lived storms from the sample: hurricanes Charley, Frances, Ivan and Jeanne from 2004, along with 2005 hurricanes Katrina, Rita, and Wilma (Fig. 8). The resulting regression equation

$$\mathrm{NHC17} = 50.0 + 0.647^{*}\mathrm{HWIND17},$$

again has a regression coefficient that is significantly different from one.

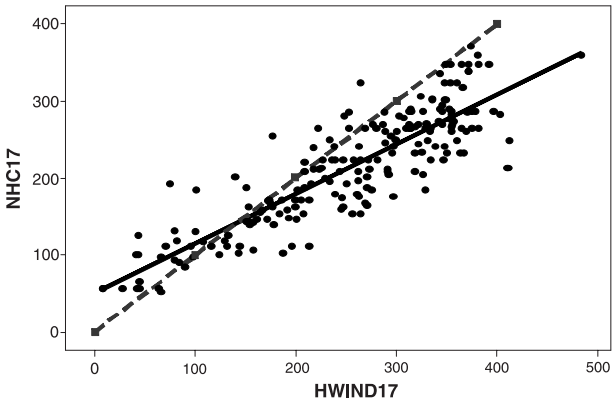

Fig. 8. Scatterplot of R_{TS} from the NHC Best Track vs. the H*Wind dataset for concurrent storm times from Hurricanes Charley, Frances, Ivan, Jeanne, Katrina, Rita, and Wilma with regression line and one-to-one line plotted. The abscissa is the H*Wind analyzed R_{TS} and the ordinate is the NHC Best Track R_{TS}. The 1-to-1 line is dashed

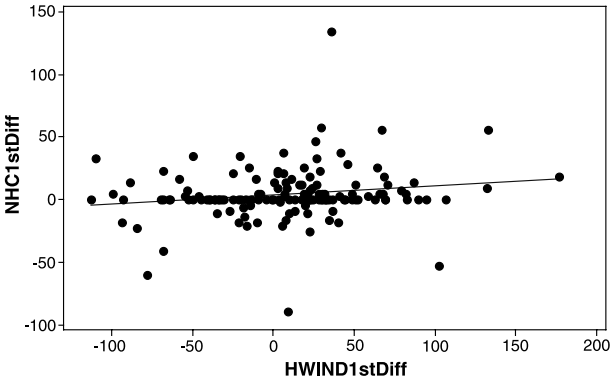

Fig. 9. Scatterplot of the first differences of the NHC Best Track (ordinate) and the H*Wind dataset (abscissa) in kilometers

Paired *t*-tests were performed on the data with only the strong, long lived storms (Table 4 middle column). For this analysis, the same pattern emerged as was found in the analysis of all storms. The entire strong, long-lived data set and all categories of hurricanes were shown to have significantly different means for the two datasets. Tropical storms were again shown to be similar in the two datasets.

A second regression analysis was performed with a dummy variable for long-lived, intense storms (1 if yes, 0 if no). If the coefficients on the dummy variable and the interaction of the dummy variable with the H*Wind gale radius variable HWIND17 are not significantly different from zero, then there is no effect from using only the long-lived, intense storms. The regression equation is now

$$\mathrm{NHC17} = 39.9 + 0.614\ \mathrm{HWIND17} + 10.1DV + 0.0330(DV^{*}\mathrm{HWIND17}),$$

where DV is the dummy variable and (DV* HWIND17) is the interaction effect. In this case, both coefficients on the dummy variable terms are not significantly different from zero, so there is no effect due to long-lived, intense storms. That is, long-lived, intense storms do not contribute disproportionately to any dataset differences.

(c) Impact of Serial Correlation

Another concern with the regression analysis is the potential effect of serial correlation reinforcing the differences between the datasets. Examination of the first differences of the NHC Best Track data reveals that much of the time there is little change in the wind radii from one time period to the next while there is more variation in the H*Wind values for R_{TS} for the same storms and storm times (Fig. 9). Given the strong tendency for little change in the NHC Best Track data, the effect of serial correlation must be addressed.

In order to evaluate if the serial correlation had an effect on the regression of NHC17 on HWIND17, a resampling analysis was performed on the data using i samples from each storm for $i = 1$ to 10 (Sect. 2). This was repeated 100 times per sample size, i. The same linear regression analysis was used on each of the new datasets. The results from these analyzes are shown in Fig. 10. Successive estimates of the slope coefficient and intercepts are stable and the extrema converge to the values obtained with the full dataset as i increases. From this analysis we conclude that estimates of significance on the differences between the H*Wind and NHC datasets were not adversely affected by the serial correlation inherent in the two datasets.

(d) Sensitivity to QuikSCAT Input Data

Detailed examination of the H*Wind dataset revealed an unexpected feature of the wind radii evolution apparent for some time periods: storm outer wind radii seemed to ‘‘breathe’’ from one observation time to the next. A time series of hurricane Ivan highlighting times when QuikSCAT satellite data was or was not available is plotted in Fig. 11. There are two areas where this breathing is noted: from 1330 UTC on September 9,

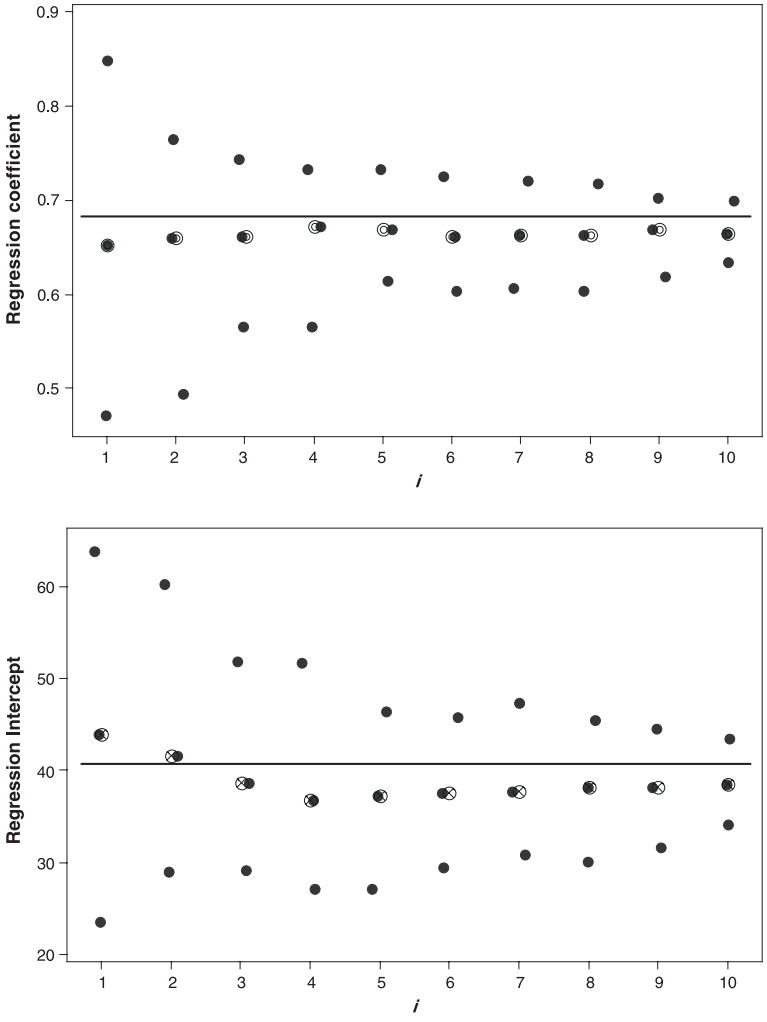

Fig. 10. Results from regression analysis of resampled datasets for the linear regression coefficient (top) and regression intercept (bottom). The top circle indicates the maximum value for the 100 resampled datasets, the middle circles designate the median and mean values (always very close in this analysis), and the bottom circle is the minimum value. The lines indicate the values for the coefficient and the intercept from the original ''all storm times'' regression analysis

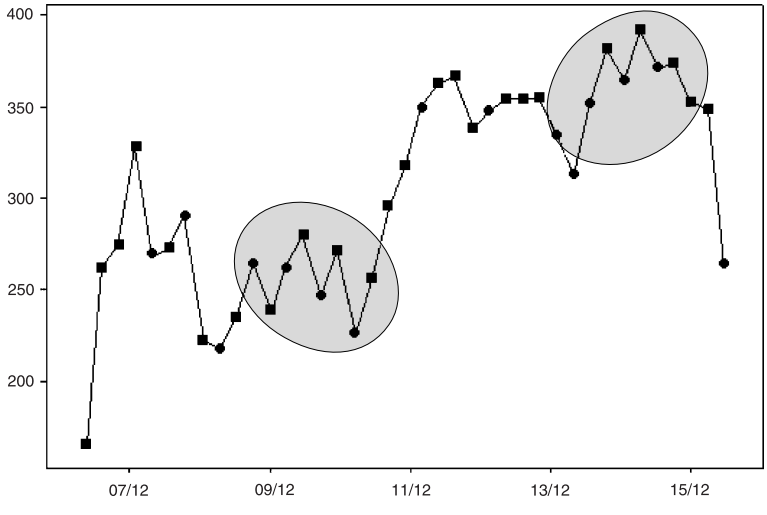

Fig. 11. Time series of average R_{TS} for hurricane Ivan. Circles indicate times when there was not QuikSCAT data available and squares indicate there was data available. The abscissa is the date and time (UTC) in September and the ordinate is R_{TS} (km). The gray shaded areas indicate where the ''breathing'' of concurrent H*Wind analyzes was noted

2004 to 0130 UTC on September 11, 2004 and from 0730 UTC on September 14, 2004 to 1630 UTC on September 15, 2004. A two-sample *t*-test was performed on the differences between NHC and H*Wind using inclusion/exclusion of QuikSCAT data as the categorical variable. None

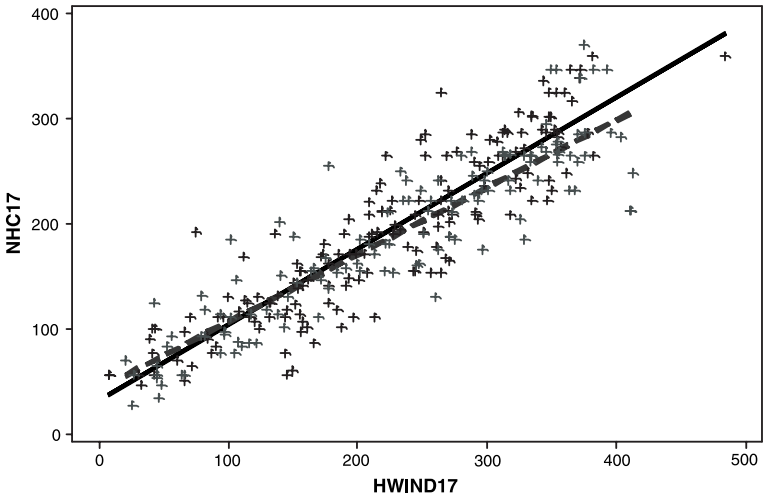

Fig. 12. Scatterplot of R_{TS} from the NHC Best Track vs. the H*Wind dataset for concurrent storm times from 2004–2005. Black crosses indicate times when there was not QuikSCAT data available and grey crosses indicate there was data available

of the *t*-tests showed statistically significant differences in the means based on whether QuikSCAT was available or not (Table 4).

Three regression analyzes were performed on the QuikSCAT data as well. The first analysis considered the entire dataset and an indicator variable was included in the regression. A scatterplot with two regression lines, one for data where QuikSCAT is available and one where it is not, is shown in Fig. 12. The lines appear to have different slopes, however the interaction term in the multiple regression is not significantly different from zero. The regression equations for the QuikSCAT analysis are:

$$\begin{aligned}\text{NHC17} &= 36.5 + 0.704\ \text{HWIND17} + 5.92\ QS \\ &\quad - 0.0640\ (QS^{*}\text{HWIND17}) \quad \text{(all)} \\ \text{NHC17\_}no &= 36.5 + 0.704\ \text{HWIND17\_}no \\ &\quad (\text{no\_}QS), \\ \text{NHC17\_}yes &= 42.4 + 0.640\ \text{HWIND17\_}yes \\ &\quad (\text{with\_}QS),\end{aligned}$$

where QS is the indicator variable and had a value of one when there was QuikSCAT in the analysis and a value of zero when there was not. The interaction term is QS^{*}HWIND17. The "*yes*" and "*no*" indicates whether QuikSCAT data was included in the analysis. The coefficients on the QS and interaction term are both not significantly different from zero. Therefore, the addition or exclusion of QuikSCAT data does not significantly affect the relationship between the H*Wind outer wind radii and NHC17.

Another way to determine if the coefficients on the independent variable are significantly different from each other is confidence intervals. Confidence intervals on the regression coefficients for the R_{TS} subsets without ("No"), and with ("Yes"), QuikSCAT data were compared. If the confidence intervals overlap, then the coefficients are not significantly different from one another. A Bonferroni correction was applied to the confidence intervals to compensate for the possibility of a Type 1 error in the hypothesis testing:

$$\begin{aligned}\beta \pm t_{0.9875,125}SE &= 0.704 \pm 2.269(0.0247) \\ &= (0.6479, 0.7600) \quad \text{(No)}, \\ \beta \pm t_{0.9875,125}SE &= 0.640 \pm 2.269(0.0271) \\ &= (0.5785, 0.7015) \quad \text{(Yes)}.\end{aligned}$$

Since there is much overlap in the confidence intervals, the two coefficients cannot be concluded to be significantly different from one another. Thus, the results of the two-sample *t*-tests and regression analyzes show that while visual inspection appeared to suggest a contribution to the bias between H*Wind and NHC wind radii due to QuikSCAT data, there is no quantitative difference in the H*Wind datasets stratified according to the presence or absence of the QuikSCAT data.

Statistical analysis of the 2004–2005 wind radii data for hurricanes available in both datasets has demonstrated that the H*Wind outer wind radii dataset is physically realistic and compares well to theory. However, there are systematic differences between the NHC Best Track and the H*Wind dataset that have yet to be resolved. One speculation was inclusion of QuikSCAT data

into the H*Wind analysis was a potential source of the differences between the two datasets. This was not supported by our analyzes. Thus, the source(s) of the differences in the NHC Best Track and H*Wind datasets are not presently identifiable.

4. Conclusions

Currently, both the H*Wind and the NHC Best Track datasets provide insight into the properties of tropical storm and hurricane surface wind distributions. Statistical analyzes of outer wind radii variations for storms observed in the 2000–2005 Atlantic hurricane seasons demonstrated that the H*Wind database is a physically realistic representation of these wind radii. Wind radii data were examined for all storms, and for storms categorized by Saffir–Simpson category. These data were further stratified by intensity change, interaction with land, and latitude. The characteristics of the H*Wind dataset examined agreed with both theory and with previous analyzes of independent Atlantic storm sets (e.g., Schwerdt et al, 1979; Ho et al, 1987).

The H*Wind dataset was not completely consistent with the other widely available wind radii dataset, NHC Best Track reanalyzes, which has also been demonstrated to be consistent with theory (Kimball and Mulekar, 2004). In a uniform comparison of concurrent analysis times for 23 storms from the 2004 and 2005 hurricane seasons, it was shown that there were statistically significant differences between the means of the two datasets for all storms and when stratified by Saffir–Simpson category. Objective estimates of R_{TS} from the H*Wind analyzes were consistently larger than the tropical storm force wind radii from the NHC Best Track reanalyzes, except for storms of only TS intensity.

To explore this systematic difference between H*Wind and the NHC Best Track wind radii, subjective estimates of outer wind radii were derived by inspection of the H*Wind analysis plots. Comparison of these subjective wind radii with the ''standard'' (i.e., objective) H*Wind outer radii values reveals that H*Wind consistently underestimates wind radii for storms when compared to the subjective estimates; the percentage underestimated increases as storm size increases. Since the resolution of H*Wind decreases further away from the center of the storm due to successively larger filter wavelengths, tests of H*Wind sensitivity to the filter wavelength and number of meshes were performed. These tests confirm that the H*Wind underestimate of wind radius is due to the smoothing associated with the objective analysis procedure. This smoothing effect is a challenge for any objective analysis technique.

There was some concern that serial correlation of R_{TS} could have influenced the regression analysis. However, through computation of 1000 subsampled regressions on resampled data, it was determined the slope and intercept obtained for the regression of NHC on HWIND were not distorted by serial correlation. Further partitioning by inclusion of QuikSCAT satellite data did not significantly change the results. Unfortunately, at this time, there is no reason to think one dataset is better than the other.

Increased satellite resolution may give assistance in assessing outer wind radii. With increases in technology, it is not out of the realm of possibility that new sensors could be added to satellites that would increase resolution and decrease rainfall attenuation in observations of tropical cyclones. Some of these measures were described by Miller et al (2006) in reference to the NexSAT program. However, the future of such high resolution satellite programs is unclear (e.g., Zielinski, 2006).

Uhlhorn and Black (2003) demonstrated that wind speed determined from the SFMR was close to wind speeds collected from near-surface GPS sondes in tropical cyclones. Since GPS sondes are the best way to measure surface parameters in-situ in an intense hurricane over water, SFMR is regarded as an effective way to measure surface wind speed. In addition, since the SFMR can be operated continually on one of the hurricane hunter aircraft, the areal extent of the observations is much larger than for GPS sondes, which only provide a point observation of the surface wind speed. If the SFMR could be flown on a WP-3 or WC-130 in the outer regions of a hurricane, ground truth for the outer wind radii would be known for that storm at that particular time. This would be especially interesting if H*Wind and NHC analyzed the outer wind radii prior to gaining knowledge of the SFMR data and then how they change once the SFMR were included. Clearly, this would not be a good ex-

periment for a landfall situation, but perhaps for a storm well out to sea, it could prove to be insightful.

Acknowledgements

The authors would like to thank Peter Black, Shirley Murillo, and Frank Marks of HRD, George Young and Jerry Harrington of Penn State Meteorology, Francesca Chiaromonte of Penn State Statistics, Mark Guishard of Bermuda Weather Service, Jessica Higgs of the Weather Channel, and Justin Arnott of NWS for their valuable insight. This work was supported by the National Science Foundation under grant ATM-0351926. This financial assistance is greatly appreciated.

References

Cocks SB, Gray WM (2002) Variability of the outer wind profiles for western North Pacific typhoons: classifications and techniques for analysis and forecasting. Mon Wea Rev 130: 1989–2005

Croxford M, Barnes GM (2002) Inner core strength of Atlantic tropical cyclones. Mon Wea Rev 130: 127–139

Demuth JL, DeMaria M, Knaff JA, Von der Harr TH (2004) Evaluation of advanced microwave sounding unit tropical-cyclone intensity and size estimation algorithms. J Appl Meteor 43: 282–296

Ho FP, Su JC, Hanevich KL, Smith RJ, Richards FP (1987) hurricane climatology for the Atlantic and Gulf Coasts of the United States. NOAA Technical Report NWS. 38, U.S. Department of Commerce, 195 pp

Kimball SK, Mulekar MS (2004) A 15-year climatology of North Atlantic tropical cyclones: Part I. Size parameters. J Climate 17: 3555–3575

Lander MA (1994) Description of a monsoon gyre and its effects on the tropical cyclones in the western North Pacific. Wea Forecast 9: 640–654

Marks F, Shay L (1998) Landfalling tropical cyclones: Forecast problems and associated research opportunities. Bull Amer Meteor Soc 79: 305–323

Ooyama KV (1987) Scale-controlled objective analysis. Mon Wea Rev 115: 2479–2506

Pennington J, DeMaria M, Williams K (2000) Development of a 10-year Atlantic basin tropical cyclone wind structure climatology [Available online at http://www.bbsr.edu/rpi/research/demaria/demaria4.html]

Pielke R Jr, Landsea C (1998) Normalized hurricane damages in the United States: 1925–95. Wea Forecast 13: 621–631

Powell MD, Houston SH (1996) Hurricane Andrew's landfall in South Florida. Part II: Surface wind fields and potential real-time applications. Wea Forecast 11: 329–349

Powell MD, Houston SH, Amat LR, Morisseau-Leroy N (1998) The HRD real-time surface wind analysis system. J Wind Eng Indust Aerodyn 77–78: 53–64

Schwerdt RW, Ho FP, Watkins RR (1979) Meteorological criteria for standard project hurricane and probable maximum hurricane windfields, Gulf and east coasts of the United States. NOAA Technical Report NWS 23, U.S. Department of Commerce, 317 pp

Uhlhorn EW, Black PG (2003) Verification of remotely sensed sea-surface winds in hurricanes. J Atmos Ocean Tech 20: 99–116

Weatherford CL, Gray WM (1988a) Typhoon structure as revealed by aircraft reconnaissance. Part I: Data analysis and climatology. Mon Wea Rev 116: 1032–1043

Weatherford CL, Gray WM (1988b) Typhoon structure as revealed by aircraft reconnaissance. Part II: Structural variability. Mon Wea Rev 116: 1044–1055

Zielinski S (2006) NASA budget focuses on exploration. EOS 87: 98

Corresponding author's address: Adam Moyer, Department of Meteorology, The Pennsylvania State University, 503 Walker Building, University Park, PA 16802, USA (E-mail: acm165@psu.edu)